

Complete On/Off Responsive ParaCEST MRI Contrast Agents for Copper and Zinc

K. Srivastava,^a† G. Ferrauto,^b† S. M. Harris,^a D. L. Longo,^b M. Botta,^c S. Aime^b and V. C. Pierre^{a*}

^a Department of Chemistry, University of Minnesota, Minneapolis MN 55455, USA

^b Molecular Imaging Center, Department of Molecular Biotechnologies & Health Sciences, University of Torino, 10126
Torino, Italy

^c Dipartimento di Scienze e Innovazione Tecnologica, Università del Piemonte Orientale “Amedeo Avogadro”, 15121
Alessandria, Italy

† Equal contributions

SUPPORTING INFORMATION

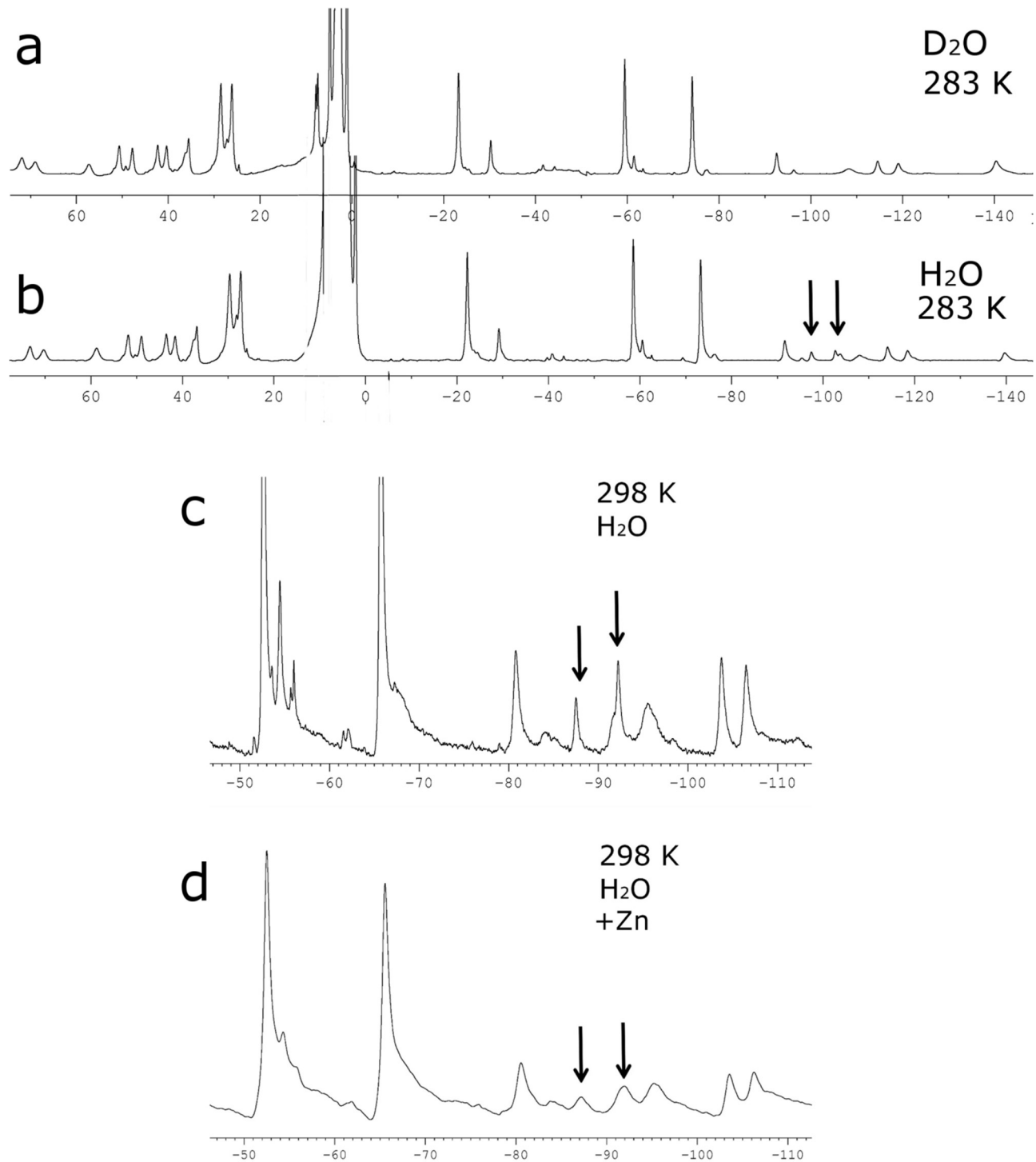


Fig. S1 a) ¹H-NMR spectra of Tm-DOTAm-py in D₂O and b) in H₂O ($B_0 = 14$ T, 10 °C, pH 7.2); c) ¹H-NMR spectra of Tm-DOTAm-py in H₂O at 298K ($B_0 = 14$ T, pH 7.2); d) ¹H-NMR spectra of Tm-DOTAm-py in H₂O at 298K in presence of one equivalent of Zn²⁺ ($B_0 = 14$ T, pH 7.2).

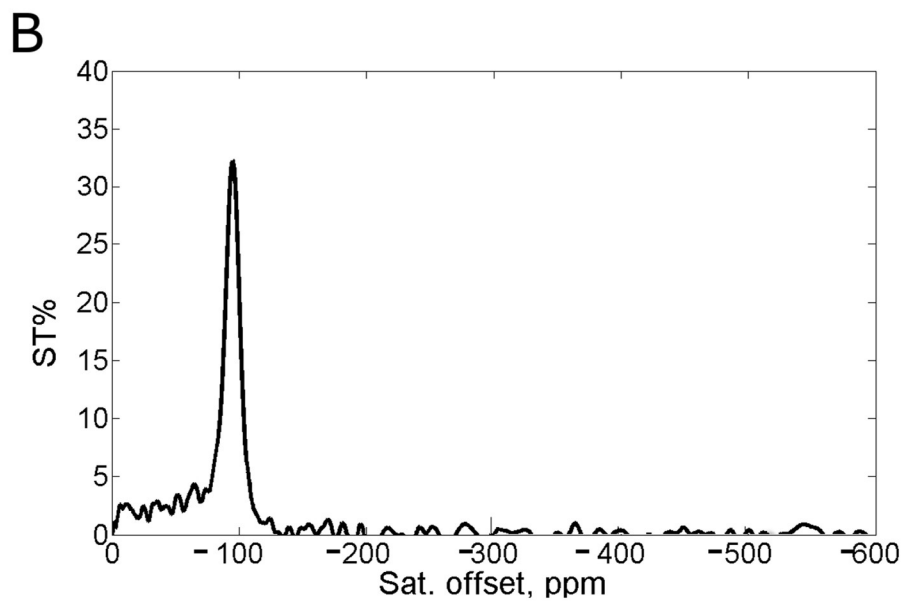
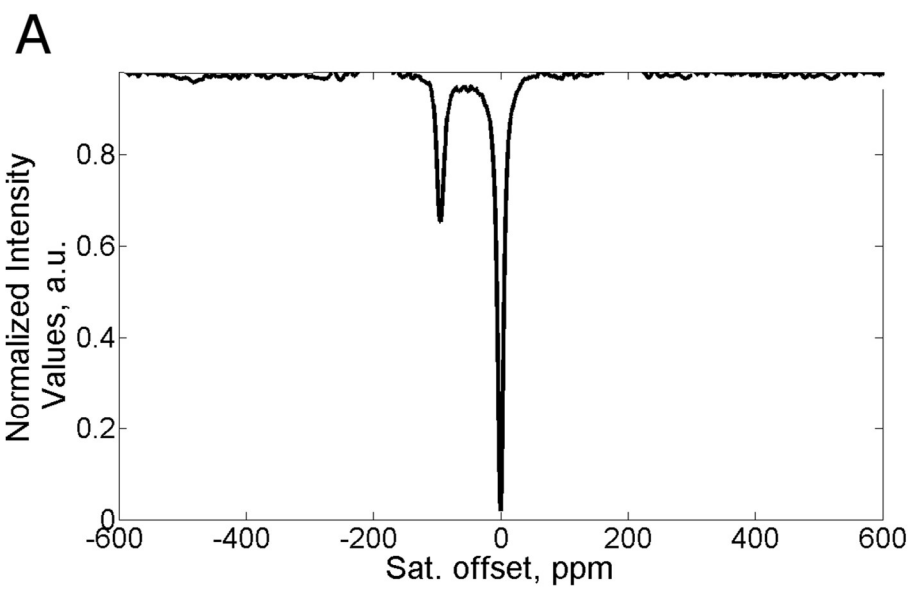


Fig. S2 a) Z- and b) ST- spectra of Tm-DOTAm-py. Experimental condition: [Tm-DOTAm-py] = 10 mM, [HEPES] = 3.8 mM, pH = 7.2, B_1 = 24 μ T, T = 21 °C.

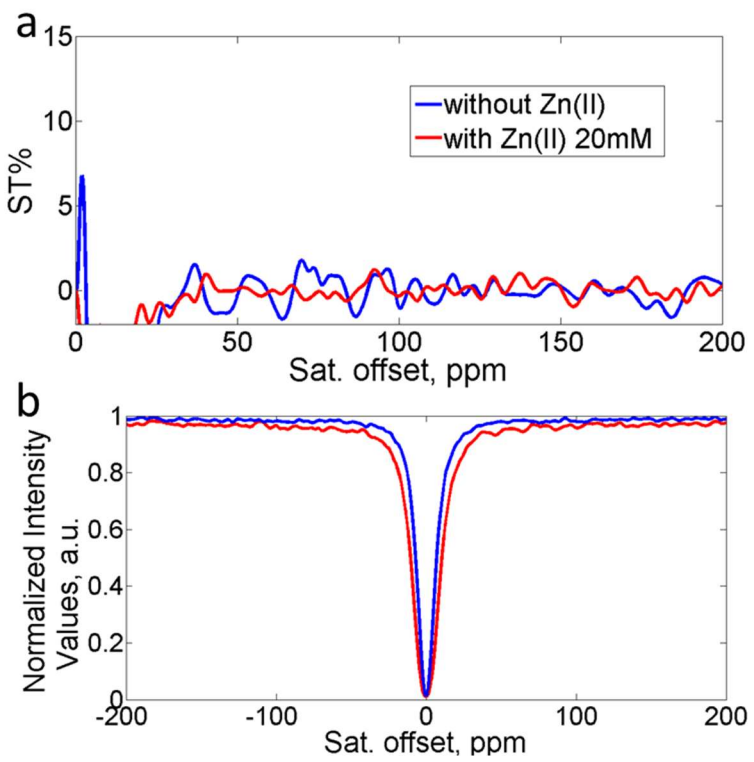


Fig. S3 a) Saturation transfer % (ST%) spectra and b) Z-spectra of Eu-DOTAm-py in the absence and presence of 20 mM ZnCl₂. Experimental conditions: [Eu-DOTAm-py] = 10 mM, [HEPES] = 3.8 mM, pH = 7.2, B_1 = 24 μ T, T = 21 °C.

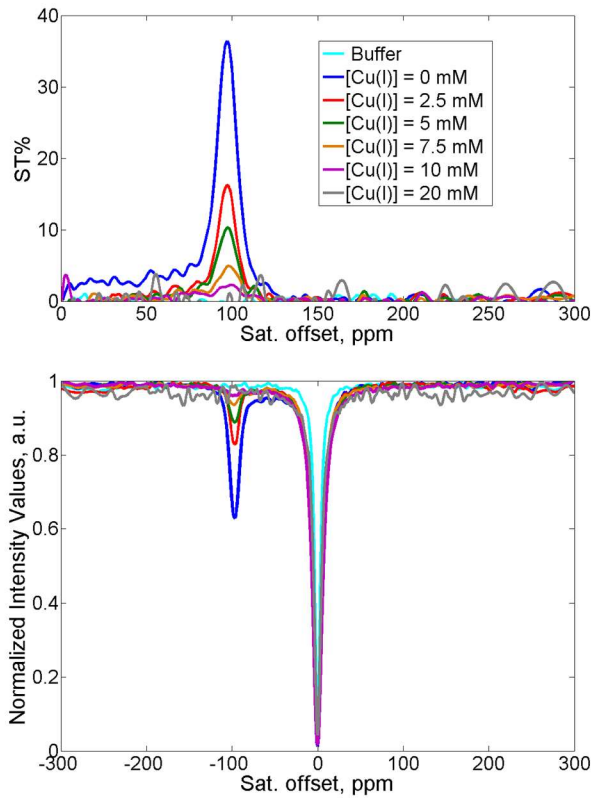


Fig. S4 a) Saturation transfer % (ST%) spectra and b) Z-spectra of Tm-DOTAm-py upon addition of different concentration of $[(\text{CH}_3\text{CN})_4\text{Cu}]\text{PF}_6$. Experimental conditions: $[\text{Tm-DOTAm-py}] = 10 \text{ mM}$, $[\text{HEPES}] = 3.8 \text{ mM}$, $\text{pH} = 7.2$, $B_1 = 24 \mu\text{T}$, $T = 21^\circ\text{C}$.

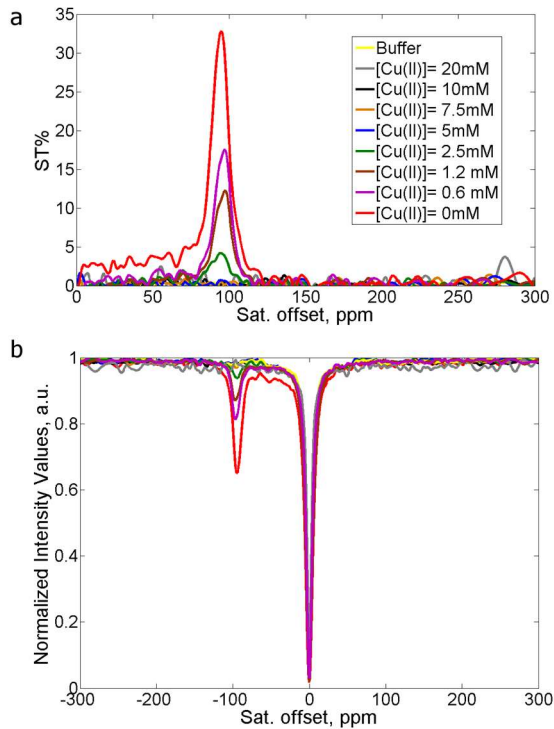


Fig. S5 a) Saturation transfer % (ST%) spectra and b) Z-spectra of Tm-DOTAm-py upon addition of different concentration of CuCl_2 . Experimental conditions: $[\text{Tm-DOTAm-py}] = 10 \text{ mM}$, $[\text{HEPES}] = 3.8 \text{ mM}$, $\text{pH} = 7.2$, $B_1 = 24 \mu\text{T}$, $T = 21^\circ\text{C}$.

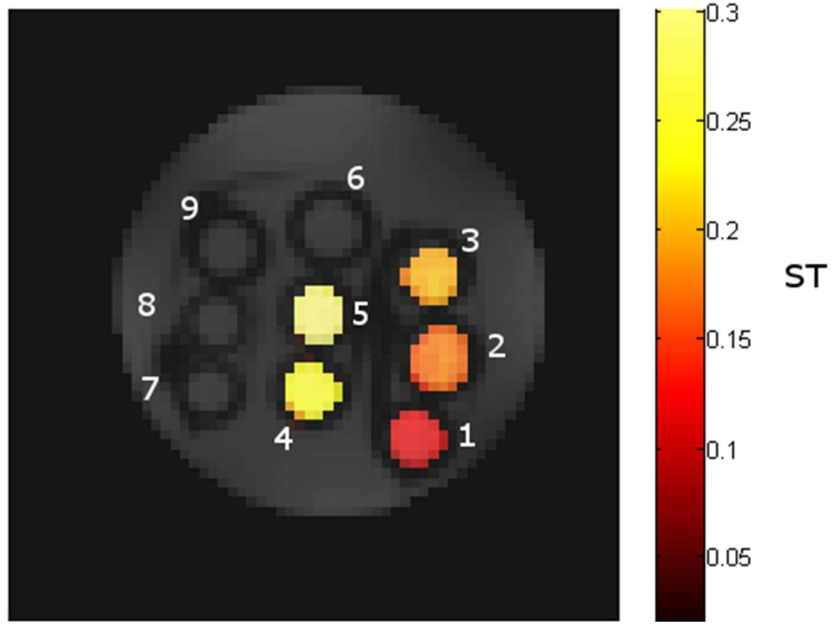


Fig. S6 CEST-MR phantom image of glass capillaries filled with aqueous solutions of 1) 10 mM Tm-DOTAm-py + 10 mM $[(\text{CH}_3\text{CN})_4\text{Cu}]\text{PF}_6$, 2) 10 mM Tm-DOTAm-py + 7.5 mM $[(\text{CH}_3\text{CN})_4\text{Cu}]\text{PF}_6$, 3) 10 mM Tm-DOTAm-py + 5 mM $[(\text{CH}_3\text{CN})_4\text{Cu}]\text{PF}_6$, 4) 10 mM Tm-DOTAm-py + 2.5 mM $[(\text{CH}_3\text{CN})_4\text{Cu}]\text{PF}_6$, 5) 10 mM Tm-DOTAm-py, 6) 10 mM $[(\text{CH}_3\text{CN})_4\text{Cu}]\text{PF}_6$, 7) 7.5 mM $[(\text{CH}_3\text{CN})_4\text{Cu}]\text{PF}_6$, 8) 5 mM $[(\text{CH}_3\text{CN})_4\text{Cu}]\text{PF}_6$, 9) 5 mM CuCl_2 , and 10) 2.5 mM $[(\text{CH}_3\text{CN})_4\text{Cu}]\text{PF}_6$. Experimental conditions: [HEPES] = 3.8 mM, pH = 7.2, T = 21 °C.

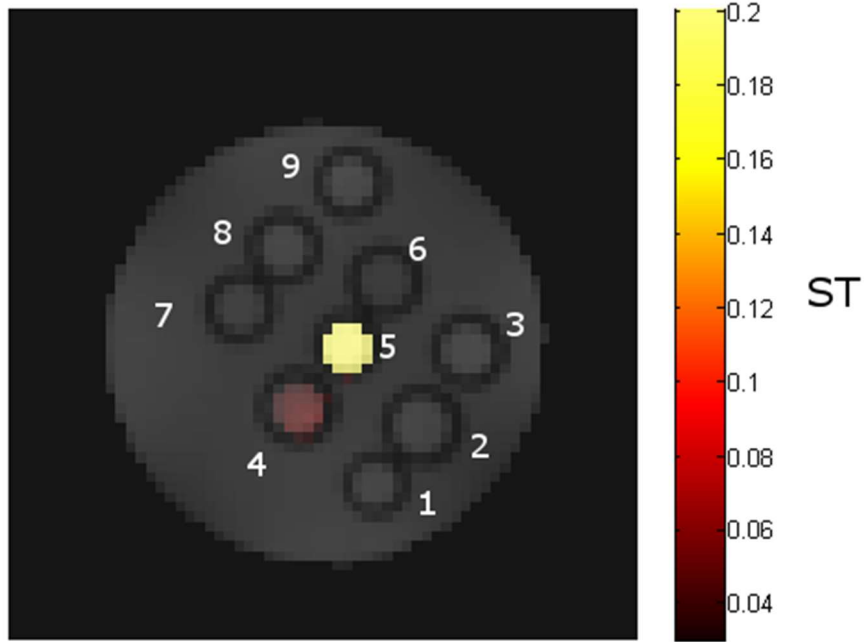


Fig. S7 CEST-MR phantom image of glass capillaries filled with aqueous solutions of 1) 10 mM Tm-DOTAm-py + 10 mM CuCl_2 , 2) 10 mM Tm-DOTAm-py + 7.5 mM CuCl_2 , 3) 10 mM Tm-DOTAm-py + 5 mM CuCl_2 , 4) 10 mM Tm-DOTAm-py + 2.5 mM CuCl_2 , 5) 10 mM Tm-DOTAm-py, 6) 10 mM CuCl_2 , 7) 7.5 mM CuCl_2 , 8) 5 mM CuCl_2 , 9) 2.5 mM CuCl_2 , Experimental conditions: [HEPES] 3.8 mM, pH = 7.2, T = 21 °C.

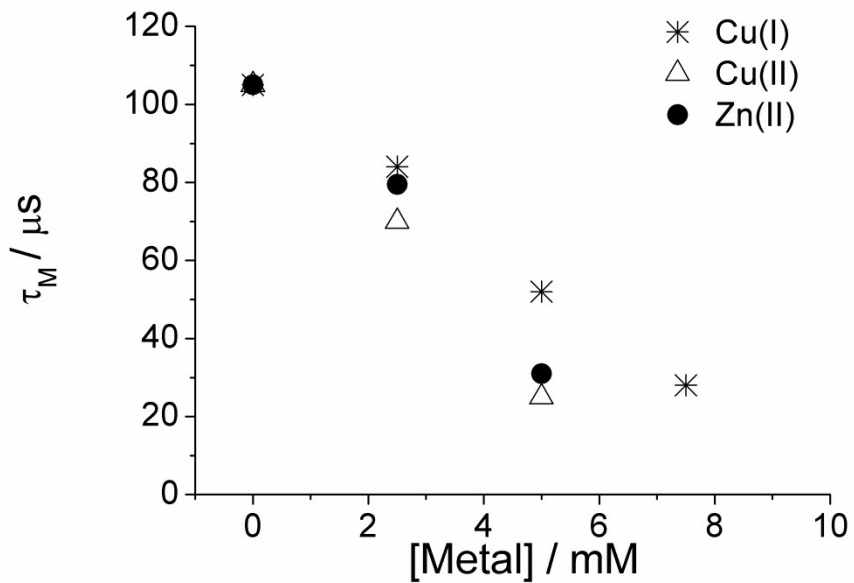


Fig. S8 τ_M of Tm-DOTAm-py upon addition of different concentration of CuCl_2 , $[(\text{CH}_3\text{CN})_4\text{Cu}]\text{PF}_6$ and ZnCl_2 . Experimental conditions: $[\text{Tm-DOTAm-py}] = 10 \text{ mM}$, $[\text{HEPES}] = 3.8 \text{ mM}$, $\text{pH} = 7.2$, $T = 21^\circ\text{C}$.

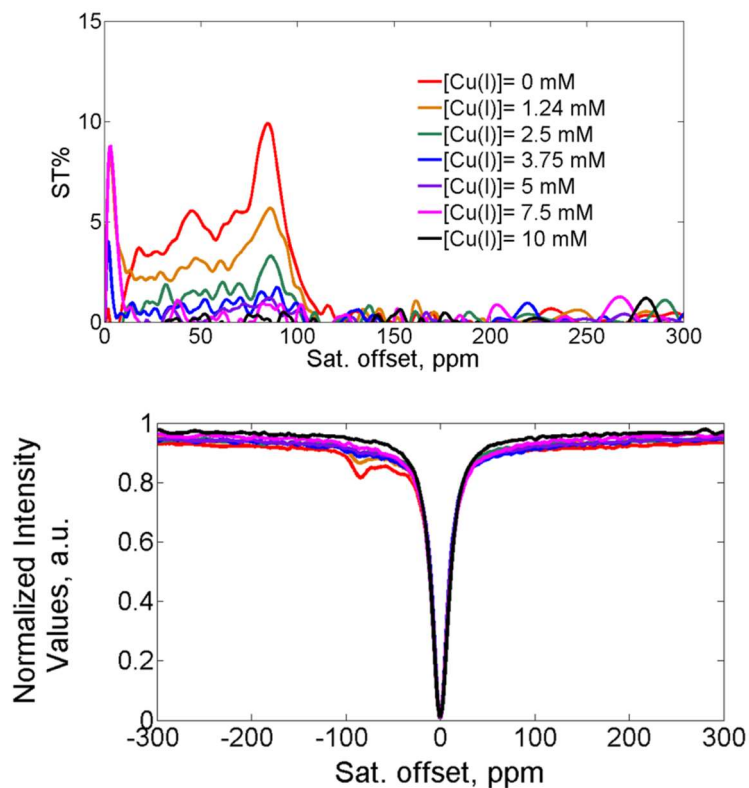


Fig. S9 a) Saturation transfer % (ST%) spectra and b) Z-spectra of Tm-DOTAm- β Ala-py upon addition of different concentration of $[(\text{CH}_3\text{CN})_4\text{Cu}]\text{PF}_6$. Experimental conditions: $[\text{Tm-DOTAm-}\beta\text{Ala-py}] = 5 \text{ mM}$, $[\text{HEPES}] = 3.8 \text{ mM}$, $\text{pH} = 7.2$, $B_1 = 48 \mu\text{T}$, $T = 21^\circ\text{C}$.

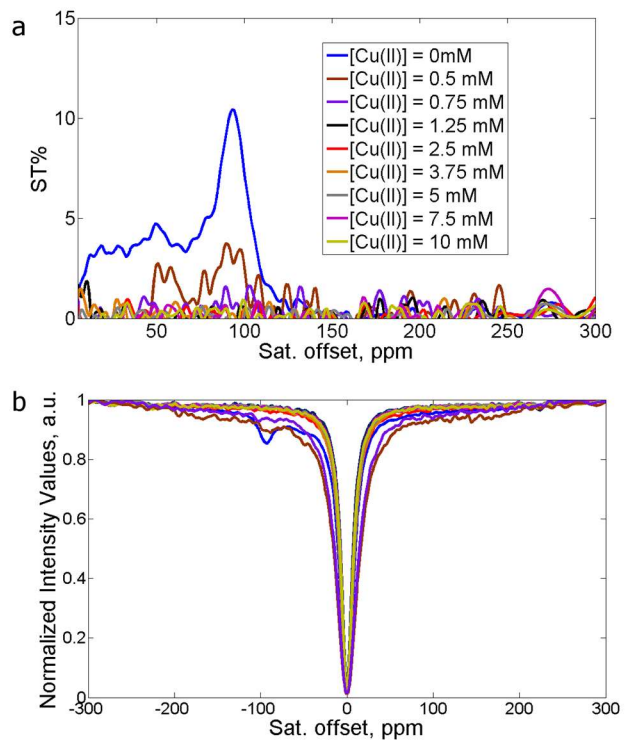


Fig. S10 a) Saturation transfer % (ST%) spectra and b) Z-spectra of Tm-DOTAm- β Ala-py upon addition of different concentration of CuCl_2 . Experimental conditions: $[\text{Tm-DOTAm-}\beta\text{Ala-py}] = 5 \text{ mM}$, $[\text{HEPES}] = 3.8 \text{ mM}$, $\text{pH} = 7.2$, $B_1 = 48 \mu\text{T}$, $T = 21^\circ\text{C}$.

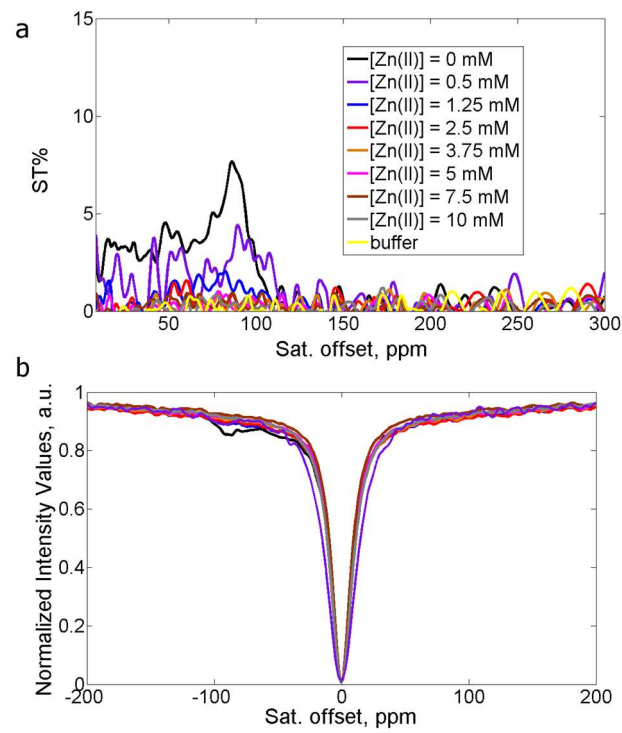


Fig. S11 a) Saturation transfer % (ST%) spectra and b) Z-spectra of Tm-DOTAm- β Ala-py upon addition of different concentration of ZnCl_2 . Experimental conditions: $[\text{Tm-DOTAm-}\beta\text{Ala-py}] = 5 \text{ mM}$, $[\text{HEPES}] = 3.8 \text{ mM}$, $\text{pH} = 7.2$, $B_1 = 48 \mu\text{T}$, $T = 21^\circ\text{C}$.

DOTAm-py

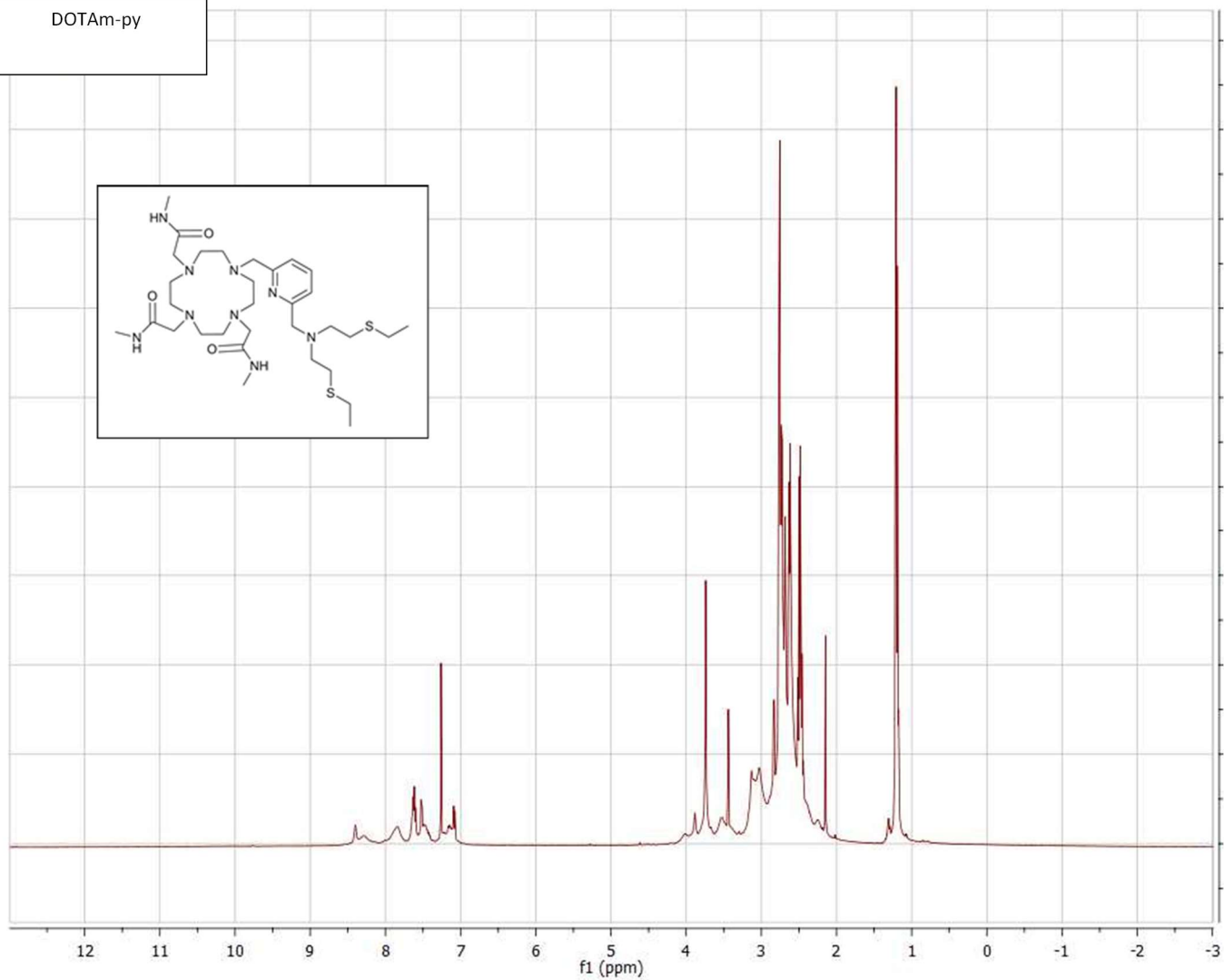
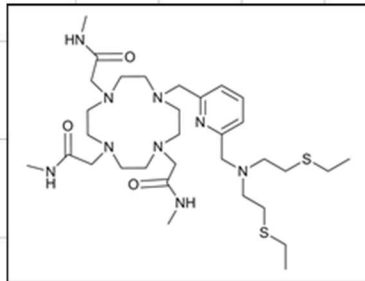


Fig. S12 ¹H NMR spectrum of DOTAm-py (CDCl₃, 500 MHz).

DOTAm-py

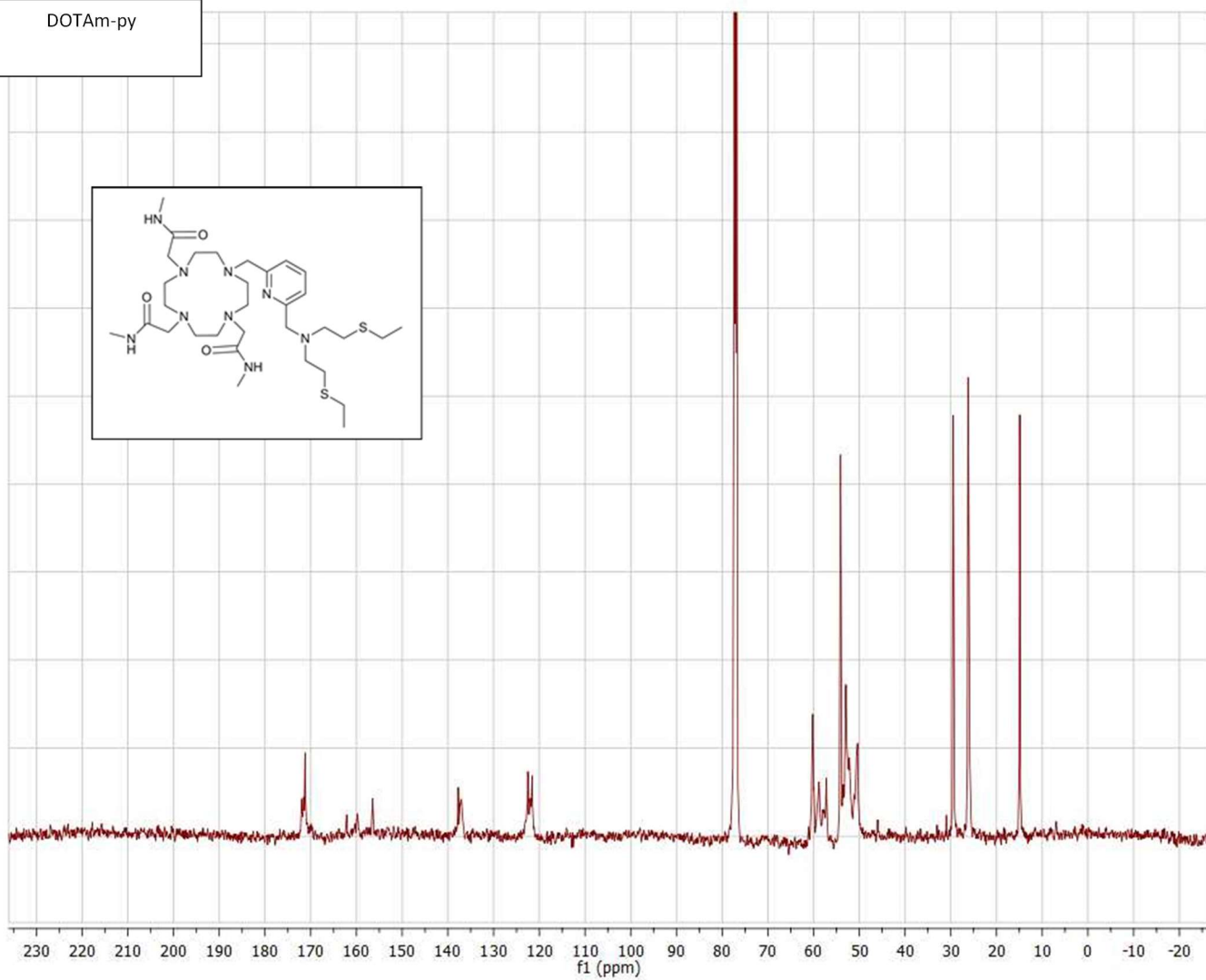
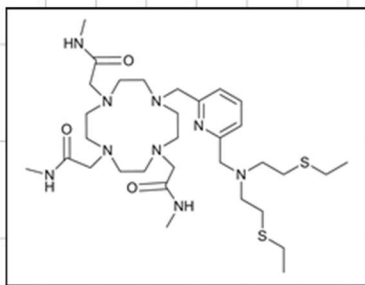


Fig. S13 ^{13}C NMR spectrum of DOTAm-py (CDCl_3 , 126 MHz).

Tm-DOTAm-py

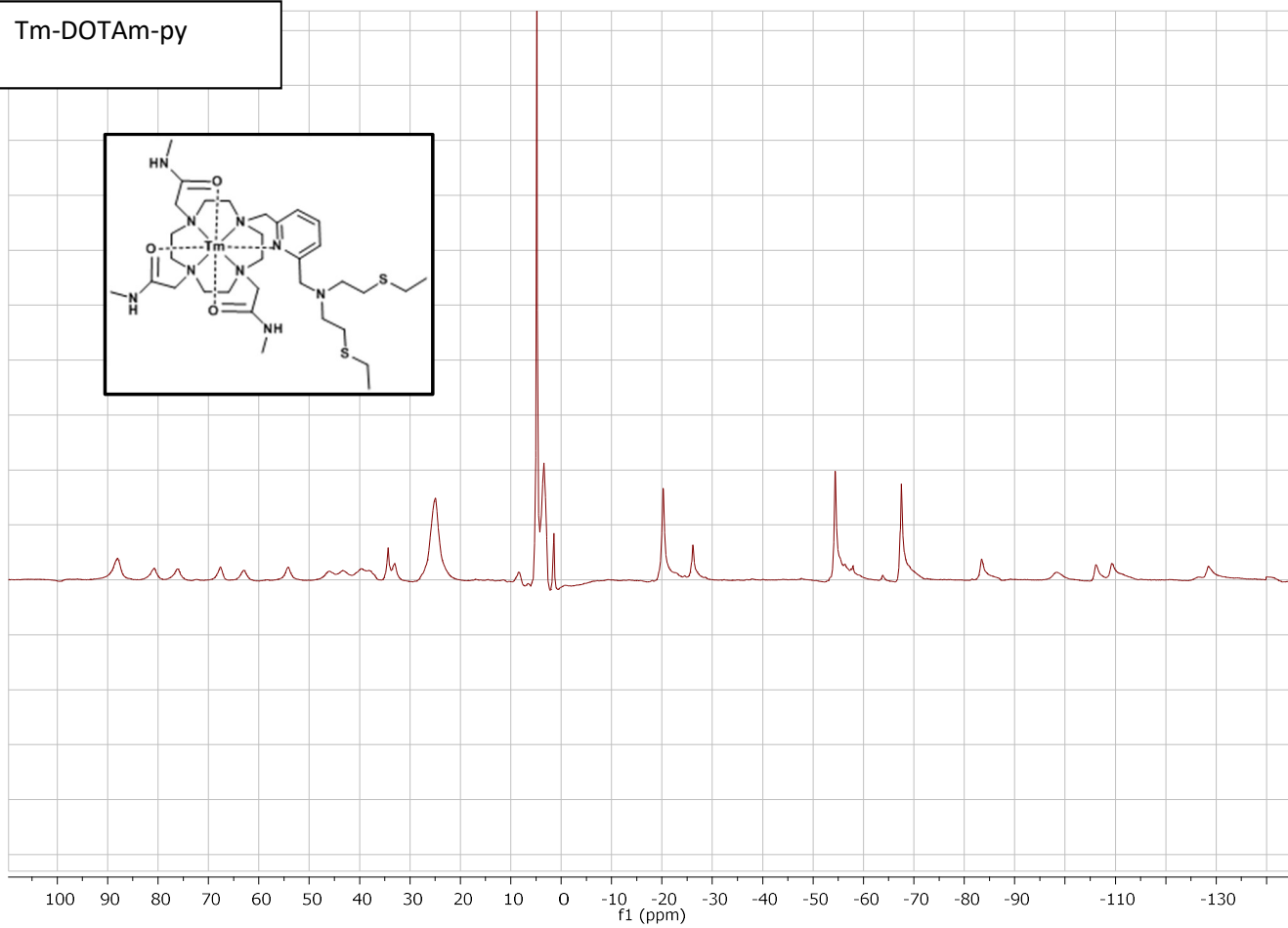


Fig. S14 ^1H NMR spectrum of Tm-DOTAm-py (D₂O, 500 MHz).

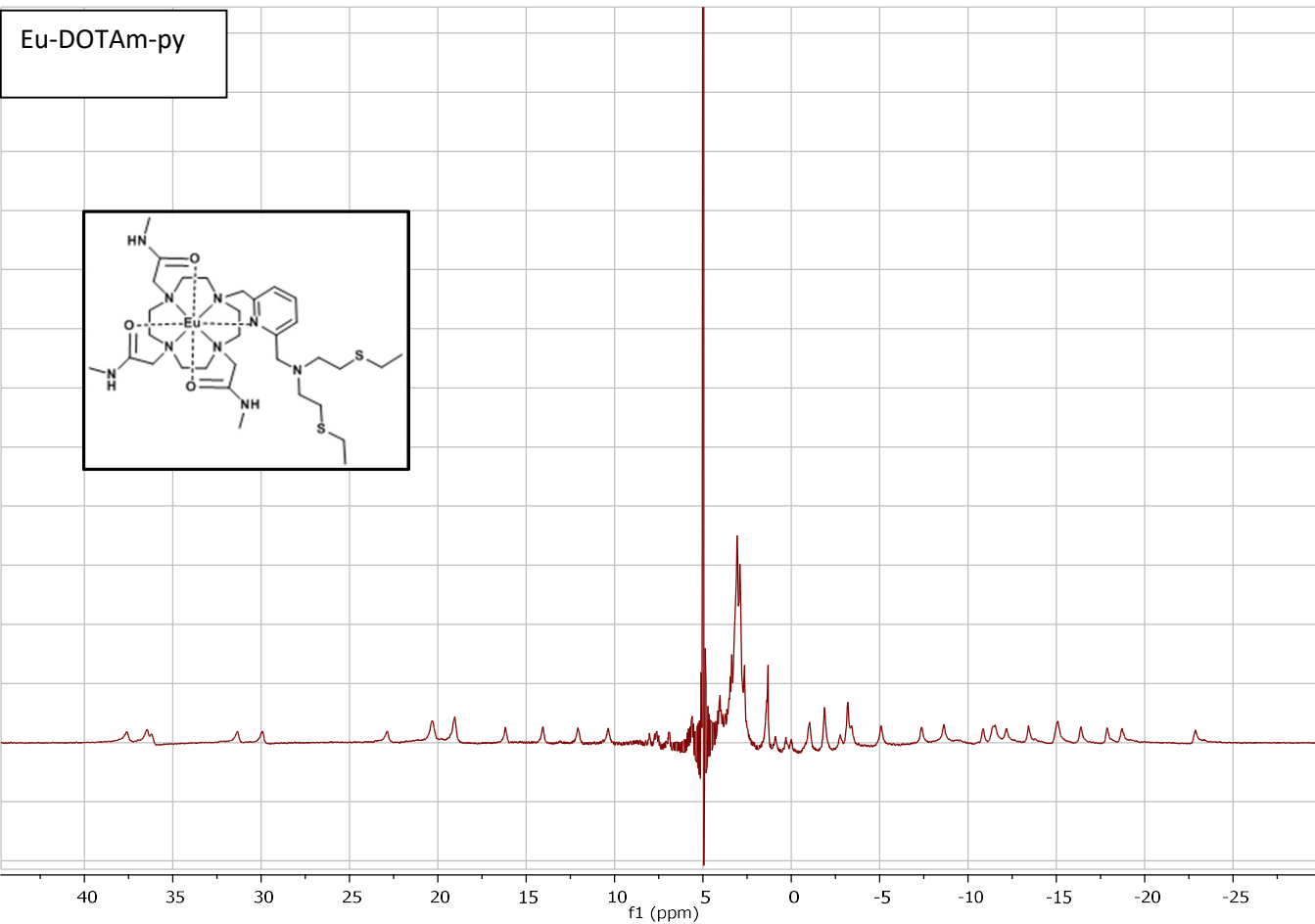


Fig. S15 ¹H NMR spectrum of Eu-DOTAm-py (D₂O, 500 MHz).

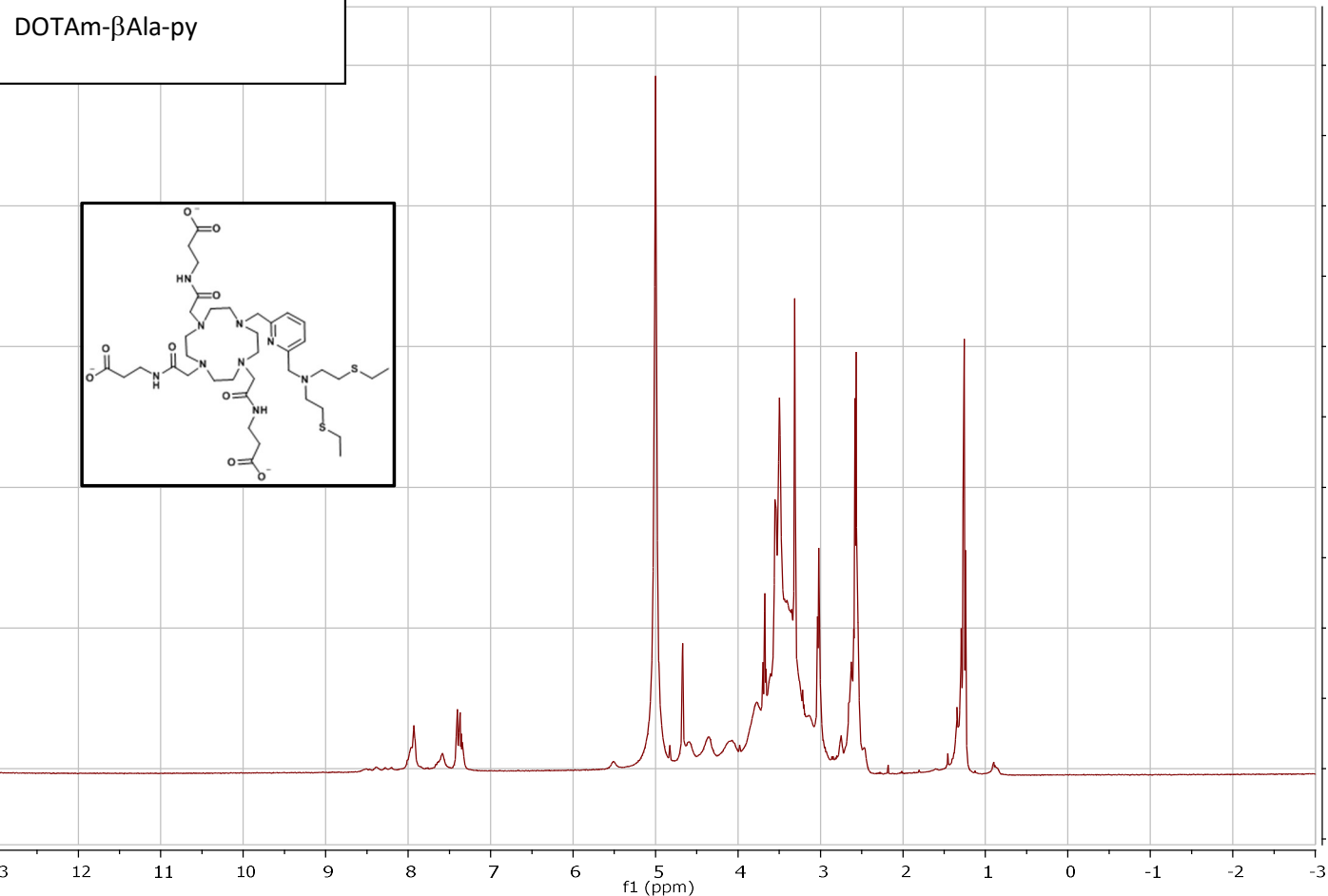


Fig. S16 ^1H NMR spectrum of DOTAm- β Ala-py (CD_3OD , 500 MHz).

DOTAm- β Ala-py

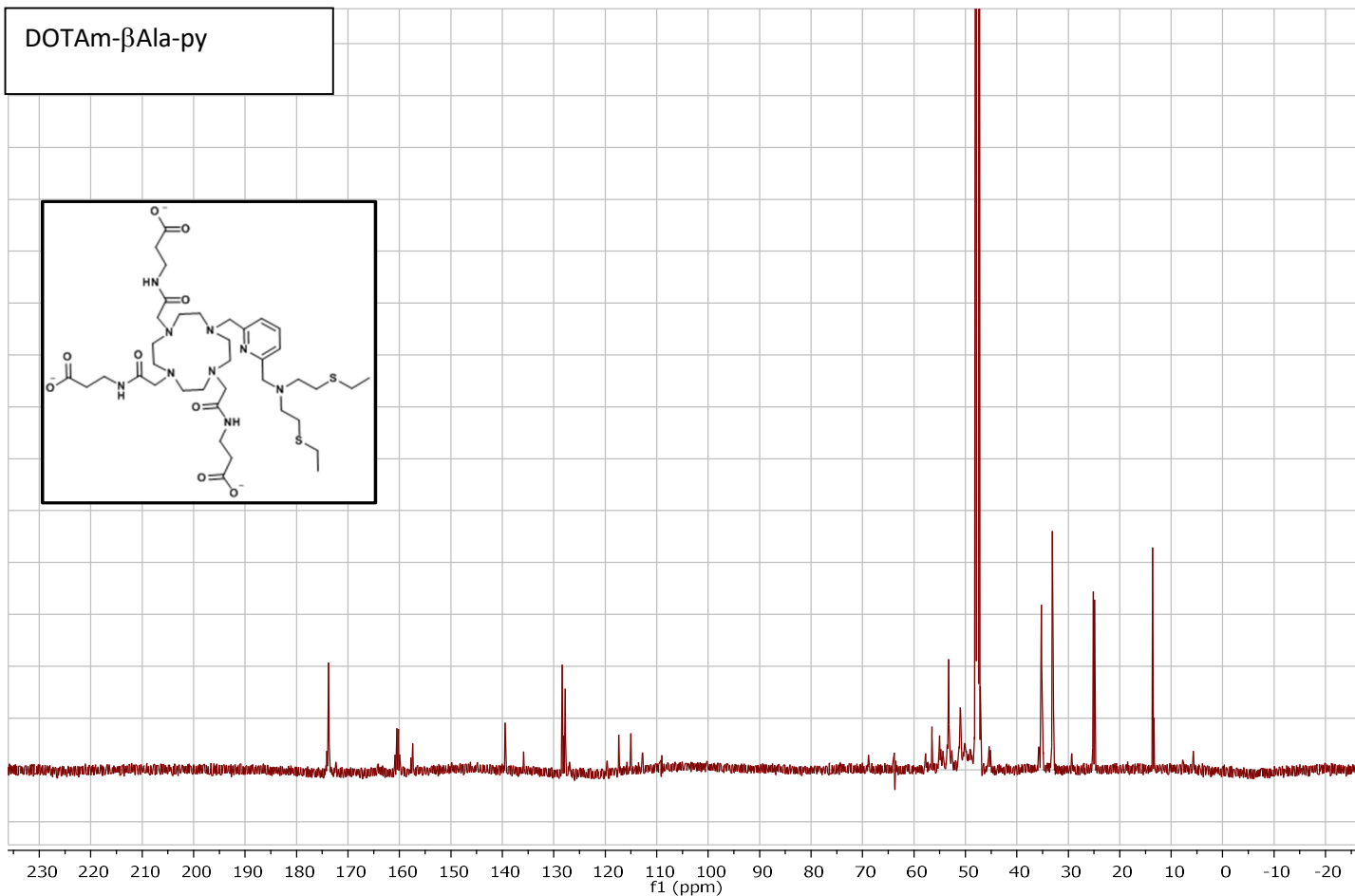


Fig. S17 ^{13}C NMR spectrum of DOTAm- β Ala-py (CD_3OD , 126 MHz).

Tm-DOTAm- β Ala-py

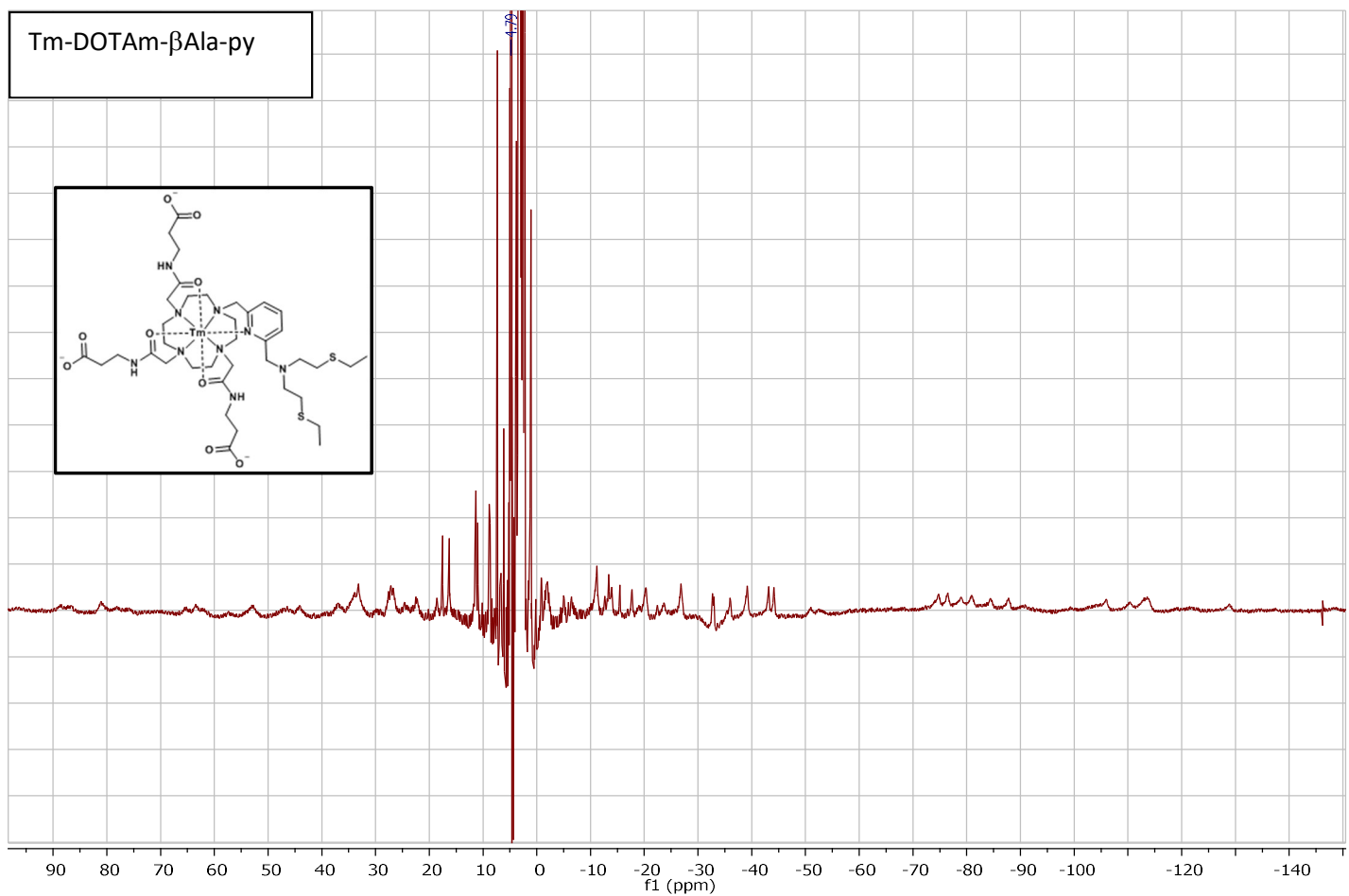


Fig. S18 ^1H NMR spectrum of Tm-DOTAm- β Ala-py (D_2O , 500 MHz).